


S.K. MOHANTY  
R.S. VERMA   
P.K. GUPTA

# Trapping and controlled rotation of low-refractive-index particles using dual line optical tweezers

Biomedical Applications Section, Raja Ramanna Centre for Advanced Technology, Indore, Madhya Pradesh, 452013 India

Received: 6 October 2006/Revised version: 16 January 2007  
Published online: 22 March 2007 • © Springer-Verlag 2007

**ABSTRACT** We show that dual line optical tweezers provides a convenient and dynamically reconfigurable approach for trapping and transport of low refractive index microscopic particles. By varying the spacing between the two line tweezers, particles of varying sizes could be trapped. Further, simultaneous rotation of the dual line tweezers could be used for controlled rotation of the trapped low-index particles. The transverse trapping force and the efficiency of the trap measured along the direction perpendicular to the line tweezers are in very good agreement with the theoretically estimated value.

PACS 07.60.-j; 87.80.Cc; 87.80.Fe

## 1 Introduction

The three-dimensional gradient force optical tweezers demonstrated by Ashkin et al. in 1986 has proven to be very useful tool for the manipulation of microscopic objects having refractive index higher than that of the surrounding medium (high index particle) [1]. Such a tweezers, however, cannot be used for trapping microscopic particles of refractive index lower than that of the surrounding medium (low index particles), because these get repelled away from the regions of the highest intensity. Low index particles such as bubbles are of considerable interest for their potential application in the field of biology and medicine. For example, recently enhancement of cell permeability caused by localized cell damage induced by the asymmetric collapse of a bubble has been used for drug delivery and transfection of genes into the living cells [2]. Since the cavitation damage by a collapsing bubble depends on its relative separation from the surface, an ability

to trap and manipulate low index particles [3] may enhance the understanding of bubble dynamics and optimize the extent of cell damage caused by bubbles. Similarly low index particles are also finding use as contrast agents [4], and for selective destruction of cancer cells [5]. One basic approach for trapping low index particles is to generate a region of lower intensity, surrounded by a higher intensity region. Several methods are being explored for this purpose, including (i) scanning a Gaussian intensity profile beam [6] in a circular path to generate a region of lower intensity, surrounded by a higher intensity region, (ii) use the optical vortex beams [7–10] or (iii) interference pattern [11]. While the scanning method is a bit complex in nature, with the use of on-axis vortex beam rotation of the trapped particles is difficult. The use of an off-axis vortex beam [12] and higher order Bessel beams [13] can overcome this difficulty. The use of a high order Bessel beam offers the advantage that the low index particle trapped in the

dark fringe region can also be rotated by transfer of orbital angular momentum from the Bessel beam [13]. However, higher order Bessel beam approach suffers from the drawback of low throughput (since the laser power is distributed in the multiple rings).

In this paper we show that dual line optical tweezers provides a convenient and dynamically reconfigurable approach for trapping and transport of low refractive index microscopic particles. This configuration, although similar in nature to that of interference pattern [11], offers two important advantages. First, in contrast with interference pattern, the spacing between the two high intensity regions can be changed independent of the width of the high intensity region. Second here all the laser beam power is distributed in only two high intensity regions whereas for interference pattern, the laser power is usually distributed in several high intensity regions. Therefore, this method can be used for efficient trapping of objects of varying sizes and can be expected to yield reasonable transverse trapping efficiency even for larger separation between the high intensity regions required for trapping larger size objects. Our measurements on the transverse trapping efficiency are consistent with these expectations. Results on controlled rotation of the trapped low-index particles by simultaneous rotation of the dual line tweezers are also presented.

## 2 Materials and method

The experimental setup (Fig. 1a) consists of a zero order

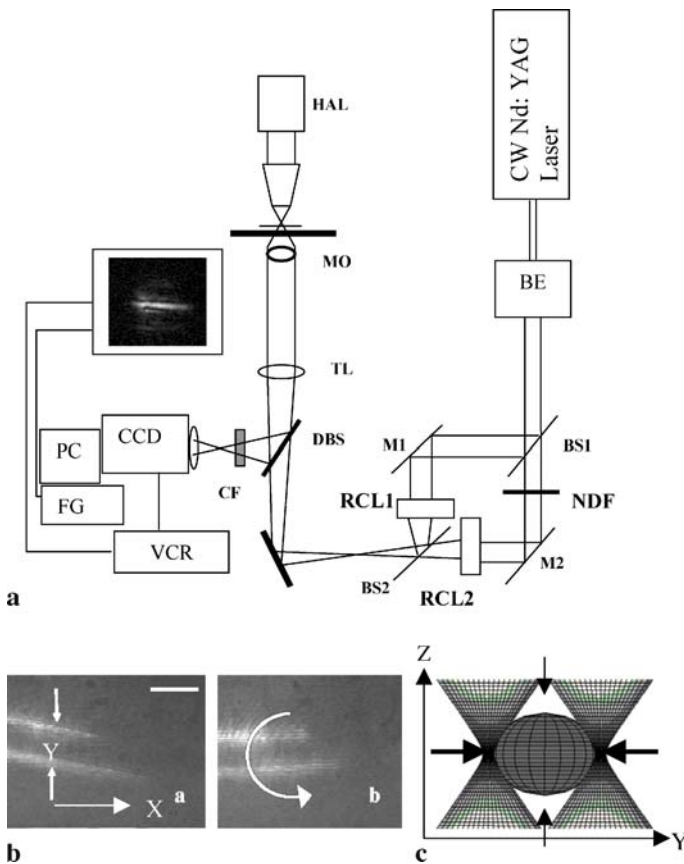


**FIGURE 1** (a) Schematic of the experimental set up. BE: beam expander; BS1-2: beam splitters; NDF: neutral density filters; MO: 100X Plan Neofluor phase objective; RCL1-2: rotating cylindrical lens; TL: spherical tube lens; HAL: halogen lamp; DBS: dichroic beam splitter; CF: IR cut-off filter (CF). (b) Simultaneous rotation of focused line profiles (a to c) by rotating the cylindrical lenses. All images are in same magnification. Scale bar: 15  $\mu\text{m}$ . (c) YZ cross-section of the simulated dual line tweezers profile showing the trapping configuration for low index particle in Y and Z directions

Hermite–Gaussian ( $\text{TEM}_{00}$ ) mode output of continuous-wave (cw) Nd:YAG laser (1064 nm; Solid State Laser Division, RRCAT) expanded using a beam expander (BE). The beam was split into two paths using a beam splitter (BS1) and neutral density filters (NDF) were inserted in one path to make the intensity of the two beams nearly equal. For generating elliptical profiles with high throughput, a cylindrical lens was used. The two beams were then combined using another beam splitter (BS2) and coupled to a 100X Plan Neofluor phase objective (MO) (N.A. = 1.3) through the base port of the microscope (Axiovert 135 TV, Carl Zeiss). The cylindrical lenses (RCL1 & 2) and the spherical tube lens (TL) of the microscope collimate the combined beam. The two laser beams were focused to elliptical spots in the specimen plane of MO and were separated by a spacing of few micrometers, by carefully tilting M1 and BS2. The two cylindrical lenses could be ro-

tated around the axis of the trap beam to cause rotation of the elliptic spots (Fig. 1b).

The motion of trapped object was recorded on a videocassette using a VCR. These images were digitized using a frame grabber and computer, and processed using software developed on LabView platform. The laser beam power at the back aperture of the objective was monitored with a power meter (Coherent Inc., USA). The low-index particle system consists of an emulsion of water droplets ( $n_p = 1.33$ ,  $\rho_p = 1.00 \text{ g/mL}$ ) in acetophenone ( $n_0 = 1.53$ ,  $\rho_0 = 1.02 \text{ g/mL}$ ). The solution was shaken vigorously to form an emulsion of spherical droplets ranging in diameter from  $\sim 50 \mu\text{m}$  down to a few  $\mu\text{m}$ . The spacing between the line tweezers was adjusted in the range of 4–30  $\mu\text{m}$  to trap particles having diameter in this range. For trapping more particles in a line, the dimensions of the line traps were extended up to 40  $\mu\text{m}$ .

### 3 Result and discussion

#### 3.1 Theoretical simulation of trapping force

The transverse profile of the z-axis directed laser beam could be expressed as

$$I(x, y, z) = \left( \frac{2P}{\pi W_1 W_2} \right) \times \exp \left( -2 \left( \frac{x - x_0}{W_1} \right)^2 - 2 \left( \frac{y - y_0}{W_2} \right)^2 \right), \quad (1)$$

where  $P$  is the power of the beam,  $W_1$  and  $W_2$  are beam width in the X and Y directions respectively. In Fig. 1c, we show the YZ cross-section of the simulated dual line tweezers profile. While the repulsive gradient force of the two line tweezers leads to the trapping of low index particle in Y-direction (minor axis of the line tweezers), trapping in Z direction is achieved by the void created by the overlap of the two diverging tweezers beam along Z-direction. The latter is also illustrated in Fig. 1c. Following the ray optics approach [14], we calculated forces on the low index particle positioned at different distances along the Y-direction from the single line tweezers for line tweezers having beam waist  $\sim 8.0 \mu\text{m}$  and  $\sim 0.4 \mu\text{m}$  at the focal plane in the X, Y direction respectively. The result is shown in panel 'a' of Fig. 2a. For these calculations the beam waist centre of the line tweezers was taken as origin. The repelling force on the low index ( $n = 1.33$ ) sphere of radius 7.5  $\mu\text{m}$  suspended in a medium with higher refractive index ( $n = 1.53$ ) is zero when the sphere is symmetrically located with respect to the center of the line tweezers. This, of course, is an unstable position as there will be equal and opposite repelling forces on the sphere. However, when such a particle is placed between two line tweezers such that it interacts with both, it will experience oppositely directed repulsive force from the two line tweezers. The particle will, thus, experience a restoring force towards the mid point of the two line tweezers. The calculated resultant forces due to the two line tweezers separated by different distances in Y direction are shown in Fig. 2a (panels b to d). For separation larger than the diameter of the particle, the particle located

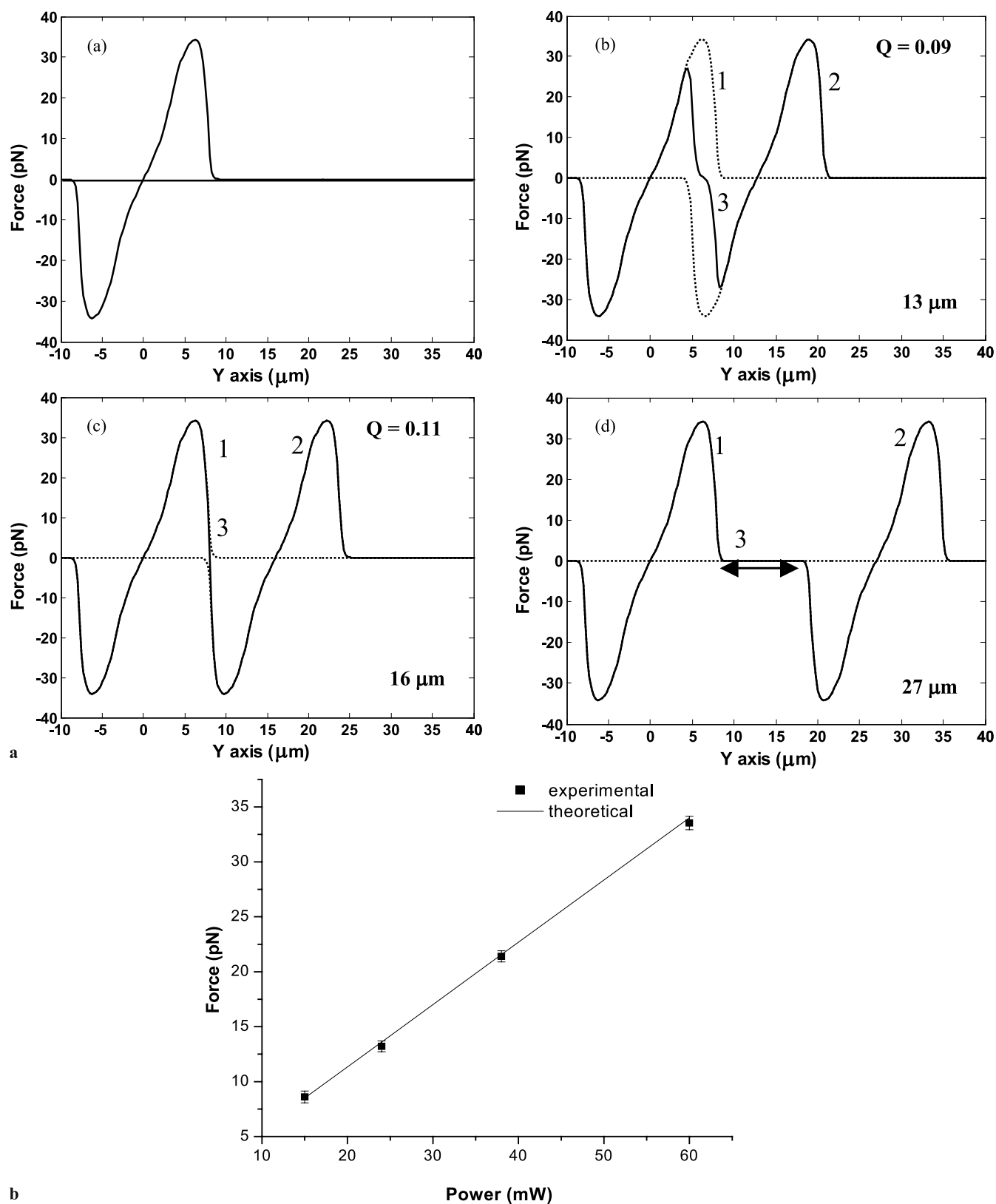


**FIGURE 2** (a) Simulated force profiles vs. position of the low-index particle (radius:  $7.5 \mu\text{m}$ ) in single line tweezers (panel a) and in dual line tweezers (panels b, c, and d). The tweezers are separated by  $13 \mu\text{m}$ ,  $16 \mu\text{m}$  and  $27 \mu\text{m}$  in panel b, c, and d respectively. The force profile due to the individual line tweezers is shown by dotted curves (1 and 2) and the resultant force due to the dual line tweezers is shown by solid curve (3). The double-sided arrow in panel d shows the interaction free region between the dual line tweezers. (b) The experimentally measured (square symbols) and the theoretically calculated trapping force (solid line) on a low-index particle (radius  $\sim 7.5 \mu\text{m}$ ) as a function of the trapping beam power. The separation between the two line tweezers was  $\sim 16 \mu\text{m}$ . The standard deviation around mean, calculated from three measurements is also shown

(the flat region shown by double sided arrow in panel d of Fig. 2a) between the two-line tweezers may not interact with the trap beam and hence will not experience any restoring force. The restoring force is maximum when the separation is close to the size of the object. The estimates for the resultant force on the particle are consistent with this expectation and reach a maximum value for separation of  $\sim 16 \mu\text{m}$ . The maximum restoring force was estimated to be  $\sim 34 \text{ pN}$  at trapping beam power of  $60 \text{ mW}$ .

### 3.2 Measurement of trapping efficiency

The escape force method was used to determine the trapping efficiency ( $Q$ ) which is related to trapping force  $F_{\text{trap}}$  by the relation,  $F_{\text{trap}} = QP/(c/n_o)$ . Here,  $P$  is the incident laser power,  $c$  the speed of light and  $n_o$  is the refractive index of the surrounding medium (here, 1.53) in which the object is trapped. In order to determine the trapping efficiency in transverse plane ( $Q_{\text{transverse}}$ ) we trapped a low-refractive index object between low intensity regions of the dual line tweezers (shown in Fig. 1c). The object was then subjected to a viscous drag by moving the specimen stage and the critical velocity of the stage,  $v_c$  at which the particle gets removed from the trap, was determined. The Stokes' law  $F_{\text{drag}} = 6\pi\eta rv$  was used to estimate drag force and equating  $F_{\text{drag}}$  corresponding to the critical velocity to  $F_{\text{trap}}$ ,  $Q_{\text{transverse}}$  can be determined in terms of  $v_c$  and  $P$ .

Using this method, the transverse trapping force  $F_{\text{trap}}$  along  $Y$  direction (perpendicular to the line tweezers) was determined, for a  $15 \mu\text{m}$  diameter particle having refractive index 1.33, as a function of the trapping beam powers. The separation between the two line tweezers was  $\sim 16 \mu\text{m}$ . In Fig. 2b we show the experimentally measured trapping force along with the theoretically estimated value. The two are in very good agreement. The trapping efficiency along the  $Y$  direction estimated from the measured transverse trapping forces was found to be  $\sim 0.11 \pm 0.02$ . It is also pertinent to emphasize here that the measured transverse trapping efficiency is an order of magnitude higher compared to trapping efficiencies reported ( $\sim 0.01$ ) for the vortex beam [9]

under similar conditions (particle size:  $10 \mu\text{m}$ ). The large value for transverse trapping efficiency primarily arises due to the fact that for the line tweezers the minor axis of the elliptical focus is much narrower than the width of the high intensity ring of vortex trap beam.

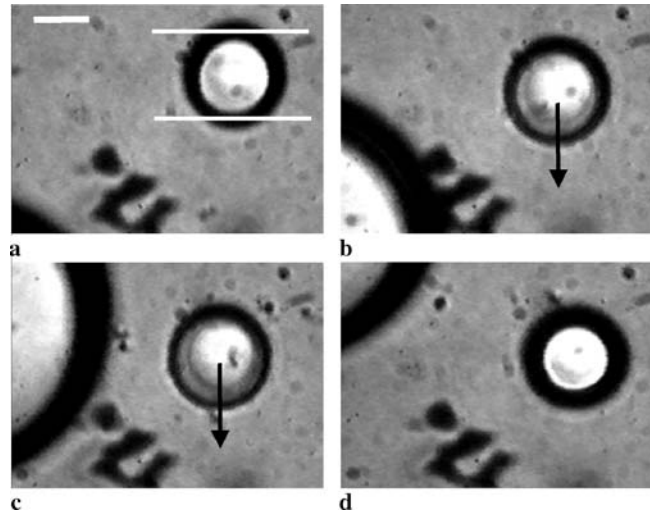
### 3.3 Transportation of low index particles

Figure 3 shows time-lapse digitized video images of trapping and transportation of low-index sphere. By translating the specimen stage, we trans-

ported the sphere trapped between two separated line tweezers (shown as straight lines) in the direction marked by arrows in panels' b to c. The sphere could also be moved up (panel d) in axial direction by translation of external cylindrical lens. As the particle diameter was  $\sim 20 \mu\text{m}$ , the spacing between line tweezers was kept  $\sim 20 \mu\text{m}$ .

### 3.4 Controlled rotation of low index particles

Figure 4 shows time-lapse digitized video images of controlled ro-



**FIGURE 3** Time-lapse digitized video images of trapping and transportation of low-index sphere. By translation of the specimen stage, the sphere trapped between two separated line tweezers (shown as straight lines in panel a) was transported in the direction marked by arrows in panel b and c. The sphere could also be moved up (panel d) in  $Z$  direction by movement of external cylindrical lens. All images are in same magnification. Scale bar:  $10 \mu\text{m}$

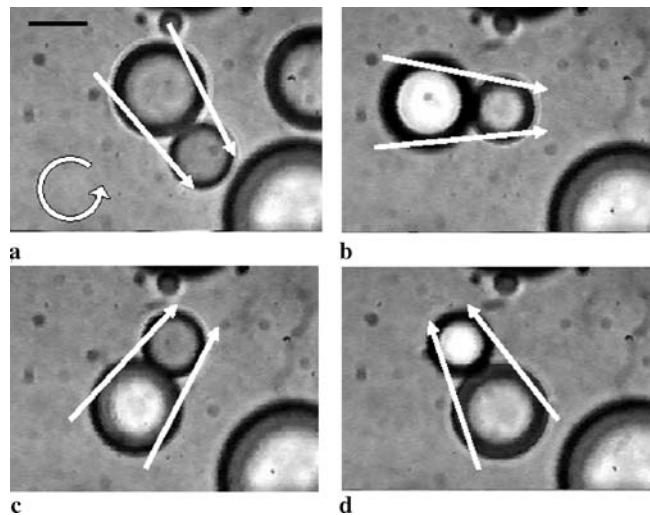


**FIGURE 4** Time lapse digitized video images of controlled rotation of low-index spheres using rotating dual line tweezers. The trapped sphere assembly between two separated line tweezers (shown as straight arrows) was rotated continuously in anticlockwise direction (marked by curved arrows) in panels a to d by simultaneous rotation of the cylindrical lenses. All images are in same magnification. Scale bar:  $5 \mu\text{m}$

tation of low-index spheres using rotating dual line tweezers. Here, since the chosen particles were having diameter between 4 to 6  $\mu\text{m}$ , the spacing between line tweezers was kept at  $\sim 6 \mu\text{m}$  on one end and  $\sim 4 \mu\text{m}$  in the other end by tilting one of the cylindrical lenses at a small angle with respect to the other. The trapped sphere assembly between the two separated line tweezers (shown as straight arrows) was rotated continuously in anticlockwise direction (marked by curved arrows) in panels a to d by simultaneous rotation of the cylindrical lenses. Both the speed and the direction could be easily controlled by the control on rotation of the cylindrical lenses. With a total power of 60 mW in both the beams, rotation speed of up to 40 rpm could be achieved. This implies that the optical torque is able to overcome the viscous drag torque ( $\tau = 8\pi\eta r^3\omega$ , where  $\omega$  is the angular velocity) of  $\sim 2.0 \pm 0.3 \text{ pN}\mu\text{m}$ . This is considerably higher than that achieved by transfer of orbital angular momentum from a high order Bessel beam [13], where a particle of similar size ( $\sim 6 \mu\text{m}$ ) and relative refractive index (1.00/1.33) could be rotated at speeds only up to  $\sim 6 \text{ rpm}$  at laser power of 600 mW. This

can be attributed primarily to the fact that the total power is distributed in the 40 rings of the Bessel beam at the focus.

#### 4 Conclusion

To conclude, we have demonstrated the use of dual line tweezers for trapping of low refractive index microscopic particles of varying sizes. Further, the trapped objects could also be rotated by simultaneous rotation of the dual line tweezers. The measured value of transverse trapping efficiency of dual line tweezers is in very good agreement with the theoretically estimated value. Apart from large trapping efficiency, which is important for trapping and orientation of sub micrometers objects, the dual line tweezers can also be used to simultaneously trap high index (in the high intensity regions [15]) and low index particles.

**ACKNOWLEDGEMENTS** Authors would like to thank H.S. Patel for many useful discussions and a careful reading of the manuscript, R. Dasgupta for providing the low refractive index samples, and members of SSLD, RRCAT for their help in smooth running of the Nd:YAG laser.

#### REFERENCES

- 1 A. Ashkin, J. Dziedzic, J. Bjorkholm, S. Chu, *Opt. Lett.* **11**, 288 (1986)
- 2 K. Tachibana, T. Uchida, K. Ogawa, N. Yamashita, K. Tamura, *Lancet* **353**, 1409 (1999)
- 3 J.Y. Ye, G. Chang, T.B. Norris, C. Tse, M.J. Zohdy, K.W. Hollman, M. O'Donnell, J.R. Baker, *Opt. Lett.* **29**, 2316 (2004)
- 4 N. de Jong, A. Bouakaz, P. Frinking, *Echocardiography* **19**, 229 (2002)
- 5 P. Prentice, A. Cuschieri, K. Dholakia, M. Prausnitz, P. Campbell, *Nature Phys.* **1**, 107 (2005)
- 6 K. Sasaki, M. Koshioka, H. Misawa, N. Kitamura, H. Masuhara, *Appl. Phys. Lett.* **60**, 807 (1992)
- 7 K.T. Gahagan, G.A. Swartzlander, *J. Opt. Soc. Am. B* **16**, 533 (1999)
- 8 K.T. Gahagan, G.A. Swartzlander, *Opt. Lett.* **21**, 827 (1996)
- 9 K.T. Gahagan, G.A. Swartzlander, *J. Opt. Soc. Am. B* **15**, 524 (1998)
- 10 P. Prentice, M. MacDonald, T. Frank, A. Cuschieri, G. Spalding, W. Sibbett, P. Campbell, K. Dholakia, *Opt. Express* **12**, 593 (2004)
- 11 M.P. MacDonald, L. Paterson, W. Sibbett, K. Dholakia, P.E. Bryant, *Opt. Lett.* **26**, 863 (2001)
- 12 W.M. Lee, B.P.S. Ahluwalia, X.-C. Yuan, W.C. Cheong, K. Dholakia, *J. Opt. A* **7**, 1 (2006)
- 13 V. Garce's-Chavez, K. Volke-Sepulveda, S. Chavez-Cerda, W. Sibbett, K. Dholakia, *Phys. Rev. A* **66**, 063402 (2002)
- 14 R.C. Gauthier, *Opt. Laser Technol.* **29**, 389 (1997)
- 15 R. Dasgupta, S.K. Mohanty, P.K. Gupta, *Biotechnol. Lett.* **25**, 1625 (2003)